Supplementary Information

Complete Solid State Photoisomeriztion of Bis(dipyrazolylstyrylpyridine)iron(II) to Change Magnetic Properties

Yuta Hasegawa, Kazuhiro Takahashi, Shoko Kume, and Hiroshi Nishihara
Department of Chemistry, School of Science, The University of Tokyo, 7-3-1, Hongo,
Bunkyo-ku, Tokyo 113-0033, Japan.
Email: nisihara@chem.s.u-tokyo.ac.jp

Contents

S–1 Materials and methods

Materials

Solvents and reagents were used as received from the commercial sources otherwise noted. (2,6-Di(1*H*-pyrazol-1-yl)pyridin-4-yl)methanol,[1] benzyl diethylphosphate,[2] and benzyltris(2-(methoxymethoxy)phenyl)phosphonium bromide[3] were synthesized according to the literature. Iron(II) tetrafluoroborate hexahydrate and zinc(II) tetrafluoroborate hydrate (the number of hydrate is 6–7) were received from Aldrich Ltd. *n*-Buthyllithium in hexane and manganese dioxide were obtained from Kanto Ltd. 1,10-Phenanthroline monohydrate (purity: 99–101%) was received from Wako Ltd. Silicagel 60 (0.040–0.064 mm) for a flash silica column was purchased from MERCH Ltd. Dichloromethane used as solvent for reactions was distilled from calcium hydride under a nitrogen atmosphere. Tetrahydrofuran used as solvent for reactions was distilled from sodium and benzophenone under a nitrogen atmosphere. Common solvents and anhydrous solvents used for syntheses and measurements were obtained from Kanto Chemical Ltd.

Measurement details

Magnetic susceptibility measurement in solid

Magnetic susceptibilities in solid were measured with an applied field of 0.5 T in the temperature range of 5–300 K at a rate of 1 K min^{-1} (sweep mode) with a Quantum Design MPMS SQUID magnetometer. An aluminum foil (Nippaku, Inc.) was used as a sample container, whose magnetic contributions were subtracted by measuring their own magnetic susceptibilities. The height of the container was 4 mm. A molar magnetic susceptibility was corrected for a diamagnetic susceptibility of *Z*-**2**, -324×10^{-6} cm^3 mol^{-1}, which was calculated from Pascal's constants.

NMR measurements and ESI-TOF mass spectrometry

^{1}H NMR and ^{13}C NMR spectra of samples were recorded with a JEOL ECX-400 spectrometer. H–H COSY, HMQC, and DEPT spectra were collected as supplements for the attribution of ^{1}H NMR and ^{13}C NMR spectra. ESI-TOF mass spectra were recorded with a Micromass LCT.

IR spectroscopy

IR spectra were recorded with a JASCO FT/IT-620V spectrometer. Potassium bromide (Nacalai Tesque, Inc.) was stored in a dry box and used as it was. All spectra were measured as KBr pellets. The pellet was fabricated as below; potassium bromide and each compound were well ground with a pestle in a mortar made of agate, then the mixture of the fine powder was palletized into a thin cylinder under vacuum and high pressure. A blank spectrum was measured by the use of clean KBr pellets as a reference sample before the measurement of each sample.

UV–vis spectroscopy in solution

UV–vis spectra in solution were recorded with a JASCO V-570 spectrometer at 295 K. Quarts cells (optical path: 1 cm) were used for the measurements. A base line was measured by the use of a sample and a reference cells filled with pure solvent before measurements. Sample solutions for measurements were prepared under an argon atmosphere.

Supply source of monochromic light for photoisomerization

Light source was supplied by a high-pressure mercury lamp (USH-500D, Ushio) and the bright lines were split by a monochromator (CT-10T, JASCO). The bandwidth of the light was 6 nm, and the light intensity was adjusted to be 2.5 mW cm^{-2} for 436 nm light for the solution samples. For the solid samples, the light was cut by UV cut filter and samples were irradiated by more than 420 nm light. The light intensity was 150 mW cm^{-2} for 436 nm light, of which bandwidth was 24 nm.

Single crystal X-ray diffraction analysis

Diffraction data were collected with a Rigaku AFC8 diffractometer coupled with the Rigaku Saturn CCD system and a rotating-anode X-ray generator. A suitable single crystal was mounted on a loop fiber with liquid paraffin. Temperatures just at the sample position were precisely determined after every measurement. The X-ray used was graphite-monochromated Mo K_{α} radiation ($\lambda = 0.71073$ Å). A numerical correction was applied with the program NUMABS.[4] The structure was solved with SIR-97[5] or SIR-2004[6] and the whole structure was refined using SHELXL-97[7] by the full-matrix least squares techniques on F^2. All calculations were performed using the WinGX-1.70.01.[8] software package. All non-hydrogen atoms were refined anisotropically. Hydrogen atoms of iron(II) complexes were located in idealized positions and were refined using a riding model with fixed thermal parameters.

Spectrophotometric titration

Spectrophotometric titration was carried out with a JASCO V-570 spectrometer to determine formation constants of iron(II) complexes at 295 K. Concentrations of iron(II) tetrafluoroborate hexahydrate in dry acetone were calibrated by 1,10-phenanthroline monohydrate. For the calibration, an MLCT band of the formed iron(II) tris(1,10-phenanthroline) complex were used, whose molar extinction coefficient (ε = 1.14(1) × 10^4 $M^{-1}cm^{-1}$ at 554 nm) was determined by quantitative addition of 1,10-phenanthroline to an iron(II) solution, and was close to that in water (ε = 1.10 × 10^4 $M^{-1}cm^{-1}$ at 510 nm).

Iron(II) ion and ligand solutions for measurements were prepared under an argon atmosphere. Iron(II) tetrafluoroborate hexahydrate in dry acetone (3 mL, typical concentration: 1.3 × 10^{-4} M) was added in a quarts cell (optical path: 1 cm). To avoid the evaporation of solvent, the cell was tightly sealed with rubber septums, Teflon tape, and Parafilm. Then, the ligand in dry acetone (typical concentration: 1.8 × 10^{-3} M) was added via a micro syringe. Aliquots (volume: 25 μL) were adjusted to be about 0.1 equivalent of iron(II) entity in a quarts cell. In each addition, the cell was carefully shuffled in order to complete the complexation reaction and to homogenize the solution. These operations were repeated until the complexation reactions were completed.

Absorption data around MLCT bands of formed complexes were exported to SPECFIT/32[9] (typical width and steps of wavelength are 100 and 10 nm). Data analysis and the determination of formation constants with respect to the formation of iron(II) complexes were carried out by the program SPECFIT/32; this procedure is based on a factor analysis and a least squares method. See the reference[9b] about a mathematical treatment for calculation of stability constants and absorption spectra, together with the associated standard errors.

S–2 Synthesis and characterization

(1) 2,6-Di(1*H*-pyrazol-1-yl)isonicotinaldehyde[10]

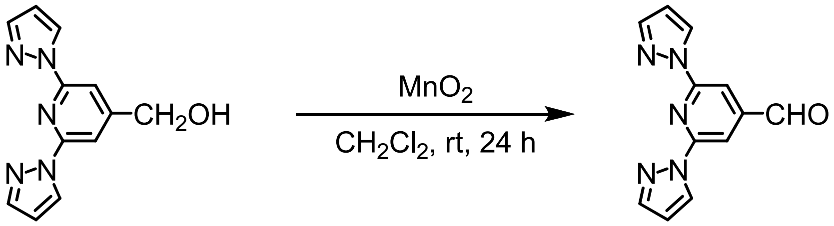

(2,6-Di(1*H*-pyrazol-1-yl)pyridin-4-yl)methanol (4.17 g, 17.3 mmol) was dissolved in 750 mL of dry dichloromethane. Manganese dioxide (94.8 g, 1.09 mol) was added to the former stirred solution, and the reaction mixture was stirred for 24 h at room temperature. And then, 100 g of silica gel was added. The reaction mixture was chromatographed on a silica column with dichloromethane–ethyl acetate (3:2) for several times to remove manganese dioxide. After manganese dioxide was completely removed, the crude product was chromatographed on a silica column with dichloromethane–ethyl acetate (3:1), and the second colorless band was collected. The product was recrystallized from dichloromethane/hexane, and was obtained as a white powder. Yield: 1.50 g (6.27 mmol, 36%). ^{1}H NMR ($CDCl_3$, 295 K): δ 10.17 (s, 1H, CHO), 8.58 (d, J = 2.8 Hz, 2H, Pz), 8.28 (s, 2H, Py), 7.81 (d, J = 1.3 Hz, 2H, Pz), 6.55 (dd, J = 2.8, 1.3 Hz, 2H, Pz). ^{13}C{^{1}H} NMR ($CDCl_3$, 295 K): δ 189.8 (CHO), 151.3 (Py), 147.1 (Py), 143.0 (Pz), 127.2 (Pz), 108.6 (Pz), 108.4 (Py). ESI-TOF mass (positive, acetonitrile): m/z = 240.14 $[M + H]^+$, calcd for $C_{12}H_{10}N_5O$, 240.09.

(2) *Z*-1

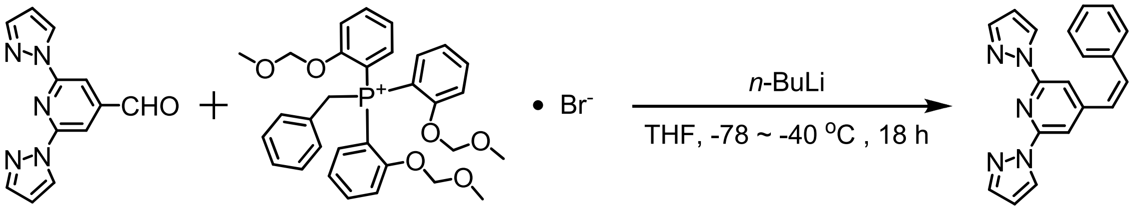

Under a nitrogen atmosphere, benzyltris(2-(methoxymethoxy)phenyl)phosphonium bromide (1.28 g, 2.09 mmol) was suspended in 75 mL of dry THF. To the former stirred solution, *n*-buthyllithium (1.59 M in hexane, 1.32 mL, 2.09 mmol) was dropwised at 0

°C. The reaction mixture was warmed to room temperature, and was turned from a white suspension to a dark-red suspension after 1 h. And then, 2,6-di(1*H*-pyrazol-1-yl)isonicotinaldehyde (500 mg, 2.09 mmol) in 75 mL of dry THF was dropwised at –78 °C. The reaction mixture was kept stirring at a temperature below –40 °C, and was turned from a dark-red suspension to a blue suspension after 18 h. After warming to room temperature, THF was removed under vacuum. The residue was suspended in 20 mL of chloroform, and filtered through *Celite* to remove lithium bromide. The filtrate, which contains *Z*- and *E*-isomers in a ratio of 8:2, was chlromatographed on a flash silica column with chloroform–acetic acid (100:0.2). The third colorless band was collected. The product was recrystallized from dichloromethane/hexane, and was obtained as white microcrystals. Yield: 320 mg (1.02 mmol, 49%). ^{1}H NMR (CD_2Cl_2, 295 K): δ 8.56 (dd, J = 2.6, 0.8 Hz, 2H, Pz), 7.71 (s, 2H, Py), 7.69 (dd, J = 1.4, 0.7 Hz, 2H, Pz), 7.34–7.26 (m, 5H, Ph), 6.89 (d, J = 12.4 Hz, 1H, CH=C*H*), 6.56 (d, J = 12.1 Hz, 1H, CH=C*H*), 6.78 (dd, J = 2.4, 1.4 Hz, 2H, Pz). ^{13}C{^{1}H} NMR (CD_2Cl_2, 295 K): δ 150.9 (Py), 150.0 (Py), 141.8 (Pz), 135.5 (Ph), 135.4 (CH=*C*H), 128.6 (Ph), 128.1 (Ph), 127.6 (Ph), 126.7 (CH=*C*H), 126.6 (Pz), 108.7 (Py), 107.4 (Pz). ESI-TOF mass (positive, acetonitrile): m/z = 314.17 $[M + H]^+$, calcd for $C_{19}H_{16}N_5$, 314.14. Analytical data. Found: C, 73.03; H, 5.02; N, 22.23%. Calcd for $C_{19}H_{15}N_5$: C, 72.83; H, 4.82; N, 22.35%

(3) ***E*-1**

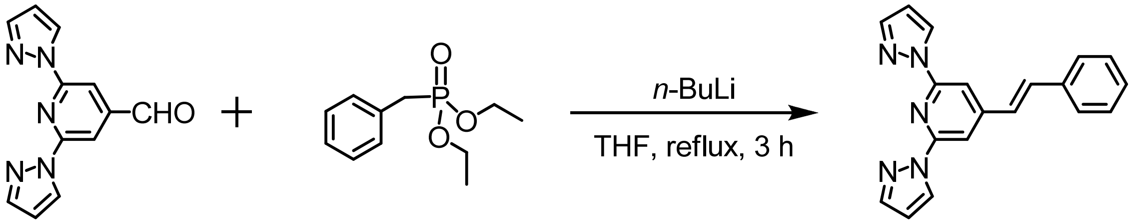

Under a nitrogen atmosphere, benzyl diethylphosphate (1.10 g, 4.81 mmol) was dissolved in 100 mL of dry THF. To the former stirred solution, *n*-buthyllithium (1.65 M in hexane, 2.92 mL, 4.82 mmol) was dropwised at 0 °C. The reaction mixture was warmed to room temperature, and the color was turned from colorless to yellow after 1 hour. And then, 2,6-di(1*H*-pyrazol-1-yl)isonicotinaldehyde (1.15 g, 4.81 mmol) in 100 mL of dry THF was dropwised at room temperature. The reaction mixture was refluxed, and was turned from yellow to orange after 3 h. After cooling to 0 °C, 200 mL of water was added to the reaction mixture, and THF was removed under vacuum. The residue, which contains *trans*- and *cis*-isomers in a ratio of 9:1, was collected, and was dissolved in a small volume of dichloromethane. The solution was chromatographed on a silica gel column with dichloromethane–ethyl acetate (5:1) as an eluent. The second colorless band was collected. The product was recrystallized from dichloromethane/hexane, to afford ***E*-1** as white microcrystals. Yield: 1.07 g (3.41 mmol, 71%). ^{1}H NMR (CD_2Cl_2, 295 K): δ 8.59 (d, J = 2.8 Hz, 2H, Pz), 7.97 (s, 2H, Py), 7.76 (d, J = 1.4 Hz, 2H, Pz), 7.60–7.58 (m, 2H, Ph), 7.53 (d, J = 16.3 Hz, 1H, CH=C*H*), 7.43–7.32 (m, 3H, Ph), 7.18 (d, J = 16.0 Hz, 1H, CH=C*H*), 6.51 (dd, J = 2.4, 1.6 Hz, 2H, Pz). ^{13}C{^{1}H} NMR (CD_2Cl_2, 295 K): δ 150.3 (Py), 150.2 (Py), 141.8 (Pz), 135.6 (Ph), 134.2 (CH=*C*H), 128.7 (Ph), 128.5 (Ph), 126.9 (Pz or Ph), 126.8 (Pz or Ph), 125.0 (CH=*C*H), 107.5 (Pz), 106.0 (Py). ESI-TOF mass (positive, acetonitrile): m/z = 314.17 $[M + H]^+$, calcd for $C_{19}H_{16}N_5$, 314.14. Analytical data. Found: C, 72.66; H, 4.99; N, 22.23%. Calcd for $C_{19}H_{15}N_5$: C, 72.83; H, 4.82; N, 22.35%.

(4) *Z*-2

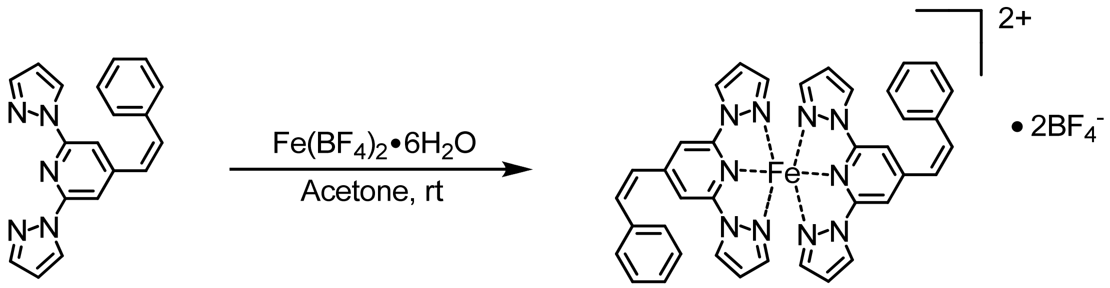

Under a nitrogen atmosphere, *Z*-**1** (174 mg, 0.556 mmol) was dissolved in 10 mL of dry acetone. $Fe(BF_4)_2 \cdot 6H_2O$ (91.6 mg, 0.271 mmol) dissolved in 4 mL of dry acetone was added to the former stirred solution at room temperature. The color of the reaction mixture immediately turned from colorless to dark-red. After stirring for 30 min, about 2/3 of the volume were slowly evaporated under a stream of nitrogen at room temperature, forming an orange precipitate. The precipitate was filtered and washed by 2 mL of ice-cold acetone. After dried under vacuum at room temperature, the product was obtained as orange microcrystals. Yield: 108 mg (0.126 mmol, 47%). ESI-TOF mass (positive, acetonitrile): *m*/*z* = 341.10 $[M]^{2+}$, calcd for $C_{38}H_{30}FeN_{10}$, 341.10. Analytical data. Found: C, 53.11; H, 3.76; N, 16.31%. Calcd for $C_{38}H_{30}B_2F_8FeN_{10}$: C, 53.31; H, 3.53; N, 16.36%. Further recrystallization of the product from nitromethane/diethyl ether afforded single crystals of *Z*-**2**.

(5) *E*-**2**

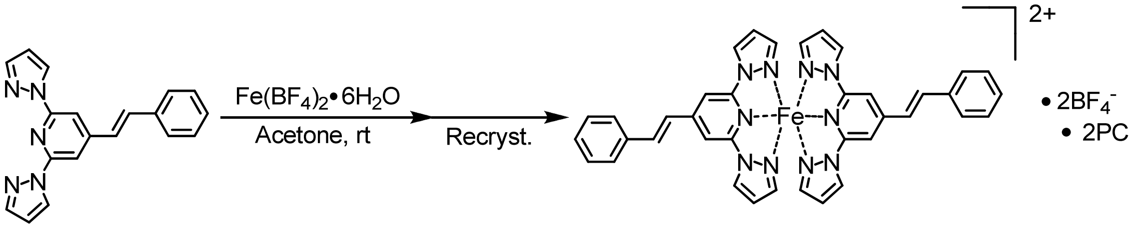

Under a nitrogen atmosphere, *E*-**1** (133 mg, 0.424 mmol) was dissolved in 10 mL of dry acetone. $Fe(BF_4)_2{\cdot}6H_2O$ (70 mg, 0.21 mmol) dissolved in 5 mL of dry acetone was added to the former stirred solution at room temperature. The color of the reaction mixture immediately turned from a colorless solution to a dark-red suspension. After stirring for 30 minutes, the precipitate was filtered and washed by 3 mL of ice-cold acetone. After dried under vacuum at 120 °C for 24 h, *E*-**2** (168 mg, 0.196 mmol, 92%) was obtained as a red powder.

Further recrystallization of the product from propylene carbonate (PC)/ethyl acetate/diethyl ether afforded single crystals of *E*-**2**·PC_2. Each crystal was collected by hand. ESI-TOF mass (positive, acetonitrile): *m*/*z* = 341.13 $[M]^{2+}$, calcd for $C_{38}H_{30}FeN_{10}$, 341.10. Analytical data. Found: C, 52.04; H, 4.20; N, 13.10%. Calcd for $C_{46}H_{42}B_2F_8FeN_{10}O_6$: C, 52.11; H, 3.99; N, 13.21%.

(6) [Zn(*Z*-1)$_2$](BF$_4$)$_2$

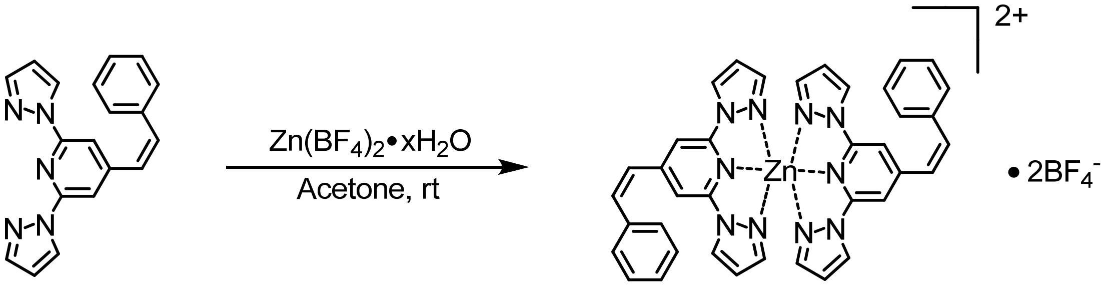

Under a nitrogen atmosphere, *Z*-**1** (100 mg, 0.319 mmol) was dissolved in 3 mL of dry acetone. Zn(BF$_4$)$_2$·xH$_2$O (x = 6–7, 55 mg, 0.15 mmol) dissolved in 3 mL of dry acetone was added to the former stirred solution at room temperature. After stirring for 30 min, about 1/3 of the volume were slowly evaporated under a stream of nitrogen at room temperature, forming a white precipitate. The precipitate was filtered and washed by 2 mL of ice-cold acetone. After dried under vacuum at room temperature, the product was obtained as white microcrystals. Yield: 52 mg (60 μmol, 40%). ^{1}H NMR (CD$_3$CN, 295 K): δ 8.32 (d, *J* = 2,8 Hz, 2H, Pz), 7.77 (s, 2H, Py), 7.55 (d, *J* = 1.4 Hz, 2H, Pz), 7.47–7.37 (m, 5H, Ph), 7.24 (d, *J* = 12.3 Hz, 1H, CH=C*H*), 6.85 (d, *J* = 12.1 Hz, 1H, CH=C*H*), 6.63 (dd, *J* = 2.8, 1.6 Hz, 2H, Pz). ^{13}C{^{1}H} NMR (CD$_3$CN, 295 K): δ 157.8 (Py), 146.3 (Py), 143.4 (Pz), 139.3 (CH=*C*H), 135.9 (Ph), 130.5 (Pz), 130.0 (Ph), 129.8 (Ph), 129.7 (Ph), 126.2 (CH=*C*H), 112.4 (Pz), 110.0 (Py). ESI-TOF mass (positive, acetonitrile): *m*/*z* = 345.09 [M]$^{2+}$, calcd for $C_{38}H_{30}N_{10}Zn$, 345.10. Analytical data. Found: C, 52.72; H, 3.66; N, 16.08%. Calcd for $C_{38}H_{30}B_2F_8N_{10}Zn$: C, 52.72; H, 3.49; N, 16.18%.

(7) [Zn(*E*-1)$_2$](BF$_4$)$_2$·H$_2$O

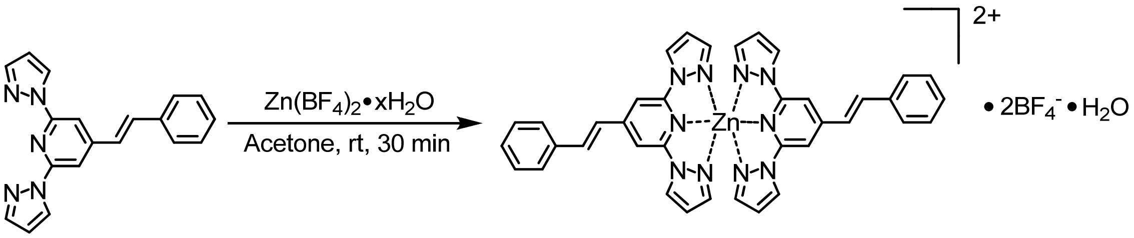

Under a nitrogen atmosphere, *E*-**1** (200 mg, 0.638 mmol) was dissolved in 10 mL of dry acetone. $Zn(BF_4)_2 \cdot xH_2O$ (x = 6–7, 110 mg, 0.31 mmol) dissolved in 7 mL of dry acetone was added to the former stirred solution at room temperature. The reaction mixture immediately turned from a colorless solution to a white suspension. After stirring for 30 min, the precipitate was filtered and washed by 5 mL of ice-cold acetone. After dried under vacuum at room temperature, the product was obtained as white microcrystals. The product had hygroscopic property. Yield: 125 mg (0.141 mmol, 45%). ^{1}H NMR (CD_3CN, 295 K): δ 8.68 (d, J = 2.3 Hz, 2H, Pz), 8.12 (s, 2H, Py), 7.97 (d, J = 16.5 Hz, 1H, CH=C*H*), 7.78 (d, J = 8.2 Hz, 2H, Ph), 7.60 (d, J = 1.8 Hz, 2H, Pz), 7.59–7.46 (m, 4H, Ph and CH=C*H*), 6.68 (dd, J = 2.3, 1.8 Hz, 2H, Pz). ^{13}C{^{1}H} NMR (CD_3CN, 295 K): δ 157.2 (Py), 146.7 (Py), 143.4 (Pz), 140.0 (CH=*C*H), 136.2 (Ph), 131.1 (Ph), 130.6 (Pz), 130.1 (Ph), 128.8 (Ph), 124.7 (CH=*C*H), 112.2 (Pz), 107.2 (Py). ESI-TOF mass (positive, acetonitrile): m/z = 345.12 $[M]^{2+}$, calcd for $C_{38}H_{30}N_{10}Zn$, 345.10. Analytical data. Found: C, 51.65; H, 3.65; N, 15.85%. Calcd for $C_{38}H_{32}B_2F_8FeN_{10}O$: C, 51.69; H, 3.59; N, 15.62%.

Table S–2–1. Crystal Data and Details for Refinement Parameters for *Z*-**2** and *E*-**2**・2PC

abbreviated name	*Z*-**2**	*E*-**2**•2PC
formula	$C_{38}H_{30}B_2F_8FeN_{10}$	$C_{46}H_{42}B_2F_8FeN_{10}O_6$
space group	*C*2/c (No. 15)	*C*2/c (No. 15)
unit cell	a = 39.672(18) Å	a = 17.211(4) Å
	b = 8.106(3) Å	b = 15.170(3) Å
	c = 36.949(18) Å	c = 19.113(4) Å
	β = 140.303(7)°	β = 111.999(3)°
unit cell vol, V	7589(6) $Å^3$	4626.9(17) $Å^3$
Z	8	4
density, ρ_{calcd}	1.498 g/cm^3	1.522 g/cm^3
abs coeff, μ	0.481 mm^{-1}	0.420 mm^{-1}
cryst color and habit	yellow plate	dark-red block
cryst size	0.31 × 0.25 × 0.02 mm^3	0.35 × 0.18 × 0.12 mm^3
temp	90(2) K	113(2) K
radiation, λ	Mo Kα, 0.71073 Å	Mo Kα, 0.71073 Å
min and max, θ	3.04 to 27.48°	3.30 to 27.47°
reflns collected	29181 [R_{int} = 0.0850]	17916 [R_{int} = 0.0525]
independent reflns	8467	5274
data/parameters/restraints	8467/553/0	5274/349/0
$R[F_0 > 4\sigma(F_0)]$	R_1 = 0.0927	R_1 = 0.0552
	wR_2 = 0.2659	wR_2 = 0.1493
GOF on F^2	1.098	1.095
max and min residual densities, e・$Å^3$	1.364, −0.834	0.865, −0.406

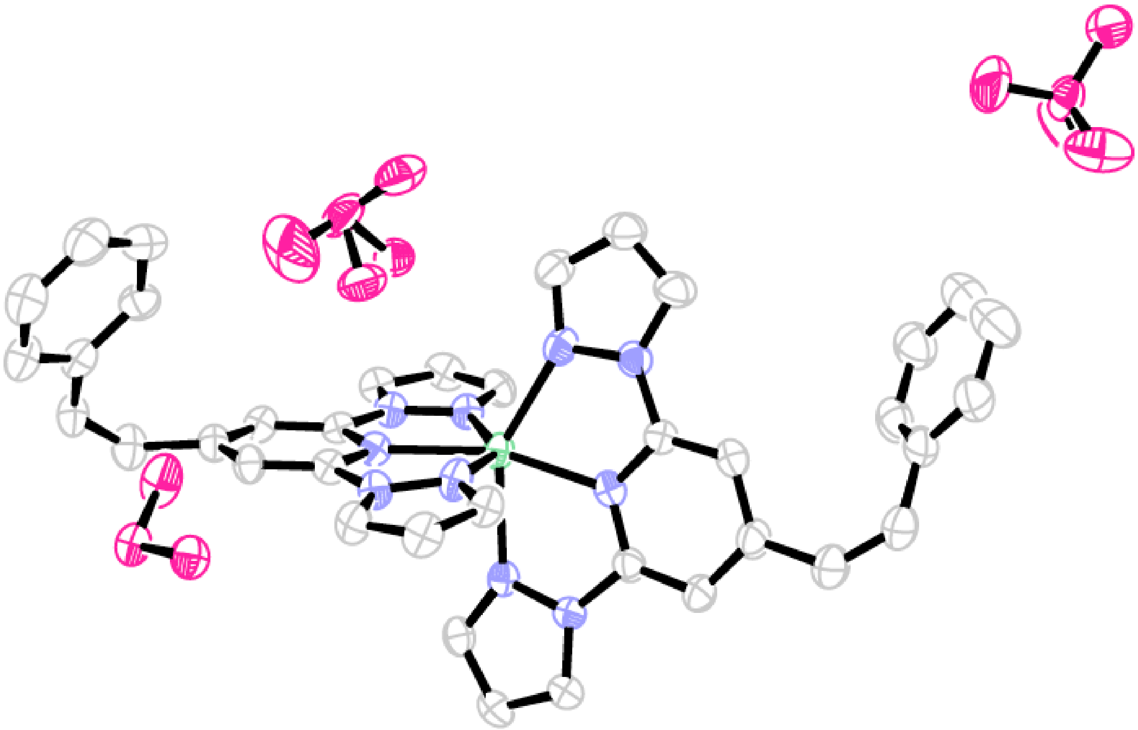

Figure S–2-1. ORTEP diagram showing 50% probability of *Z*-**2** at 90 K. Hydrogen atoms are omitted for clarity.

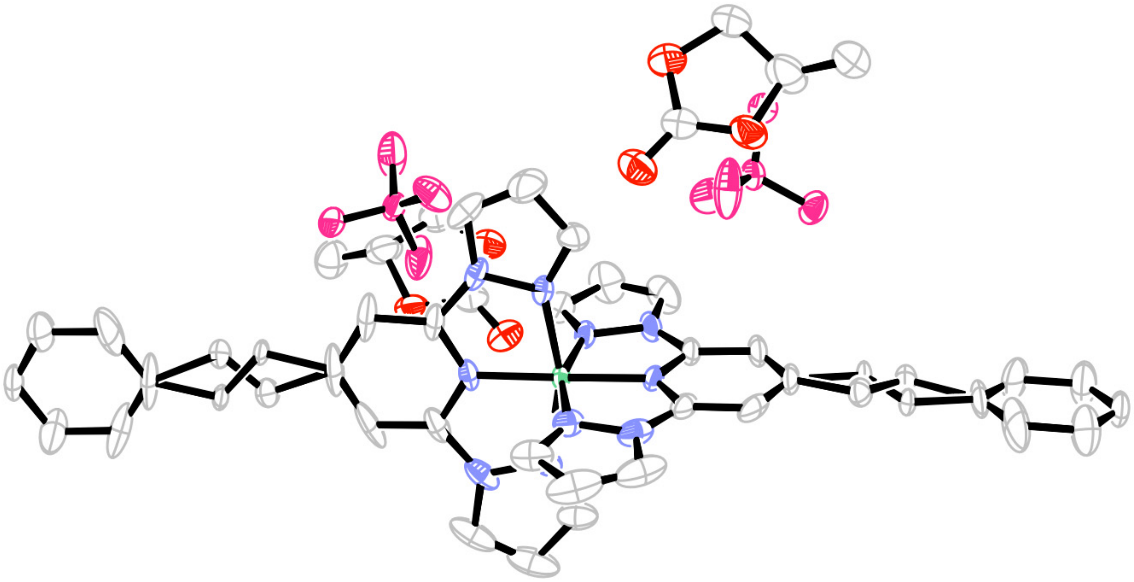

Figure S–2-2. ORTEP diagram showing 50% probability of *E*-**2**·2PC at 113 K. Hydrogen atoms are omitted for clarity.

S–3 Spectrophotometric titration

Spectrophotometric titration of $Fe(BF_4)_2 \cdot 6H_2O$ with *Z*-**1** and *E*-**1** were carried out to investigate their complexation behaviors toward an iron(II) ion. Overall formation constants of these ligands are listed in ***Table S-3-1***, and changes in UV–vis spectra and corresponding distributions of the relating species as a function of added equivalents of the ligands are shown in ***Figure S–3–1*** and ***S–3–2***.

For all cases, absorbance in the visible region, attributed to MLCT bands from formed complexes, increased accompanied by additions of ligands, and absorbance took maximum value at around 2 equivalents of ligands. Above observation suggests that Fe^{2+}:Ligand = 1:2 complex forms as the main product under the condition of existence of abundant ligands. In fact, the data can not be well fitted when a 1:3 complex are considered. These results deny the existence of the 1:3 complex, which is known to form in 2,6-bis(benzimidazol-2’-ylpyridine).[11]

Formation constants of *Z*-**1** and *E*-**1** are the same as those of dpp within the error range. This result reveals that not only isomeric states but a substituent effect of a styly moiety do not obviously affect on a complexation ability toward an iron(II) ion. When 2 equivalents of these ligands are added under experimental conditions of the spectrophotometric titration, percentages of the formed 1:2 complexes are about 95%. The value is improved to 99.9% when 3 equivalents of the ligand are added. Consequently, an excess free ligand should be added to a solution of the complex for the precise investigation of its property.

Table S–3–1. Overall Formation Constants of the Ligands to an Iron(II) ion

Ligand	Percentage[a]	Overall formation constant	
		β_{11}	β_{12}
Z-**1**	95	7.04(16)	13.5(2)
E-**1**	96	7.40(17)	14.2(3)

[a] The percentage of the formed 1:2 complex when 2 equivalents of the ligands are added under the experimental condition.

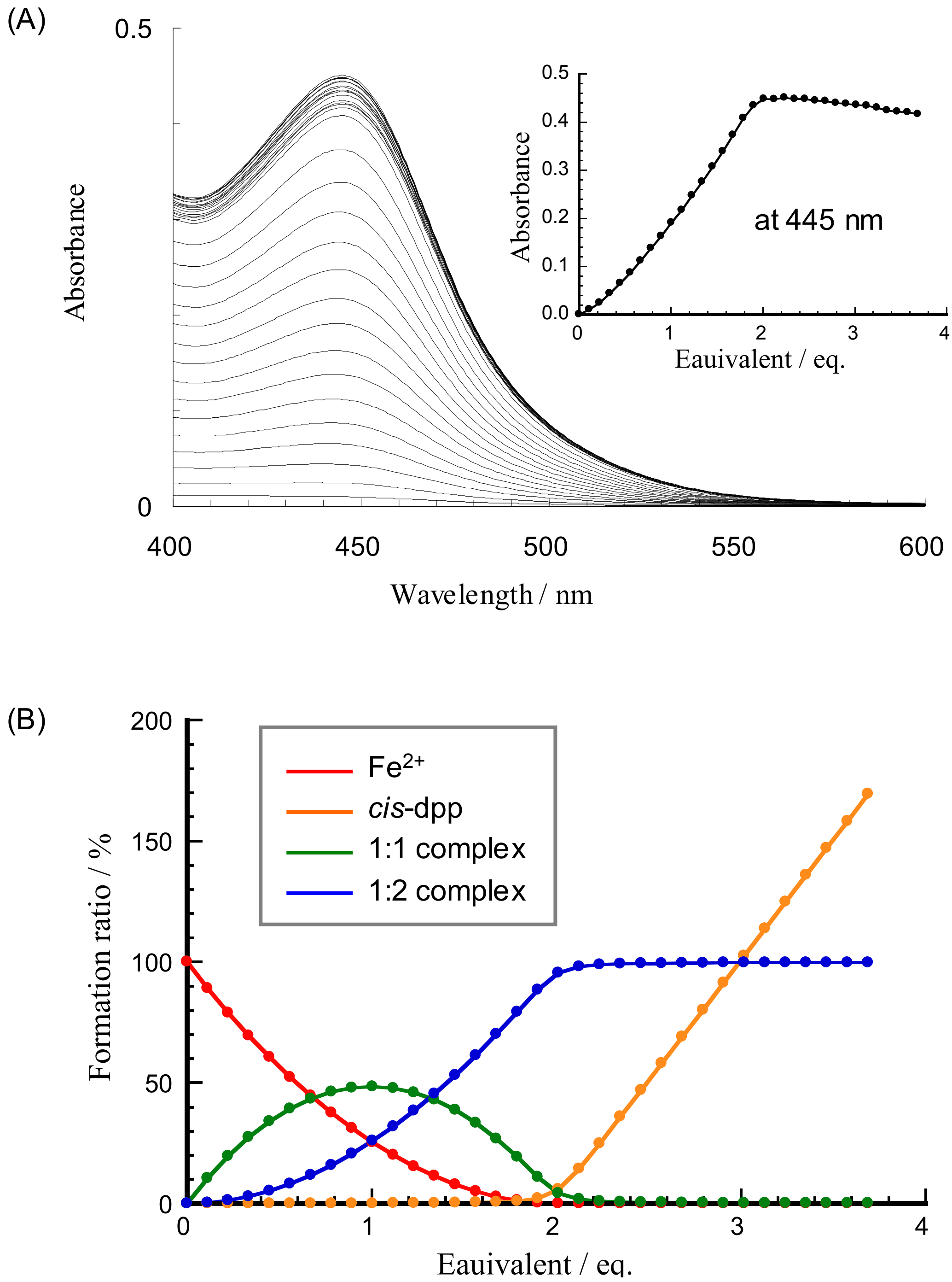

Figure S–3–1. (A) Spectrophotometric titration of $Fe(BF_4)_2{\cdot}6H_2O$ with *Z*-**1** in acetone. The concentration of $Fe(BF_4)_2{\cdot}6H_2O$ is 1.34×10^{-4} M and of *Z*-**1** is 1.80×10^{-3} M. Inset: absorbance at 500 nm as a function of added equivalent of the ligand. (B) Corresponding distributions of Fe^{2+} (red), *Z*-**1** (orange), 1:1 complex (green), 1:2 complex (blue) as a function of added equivalents of the ligand.

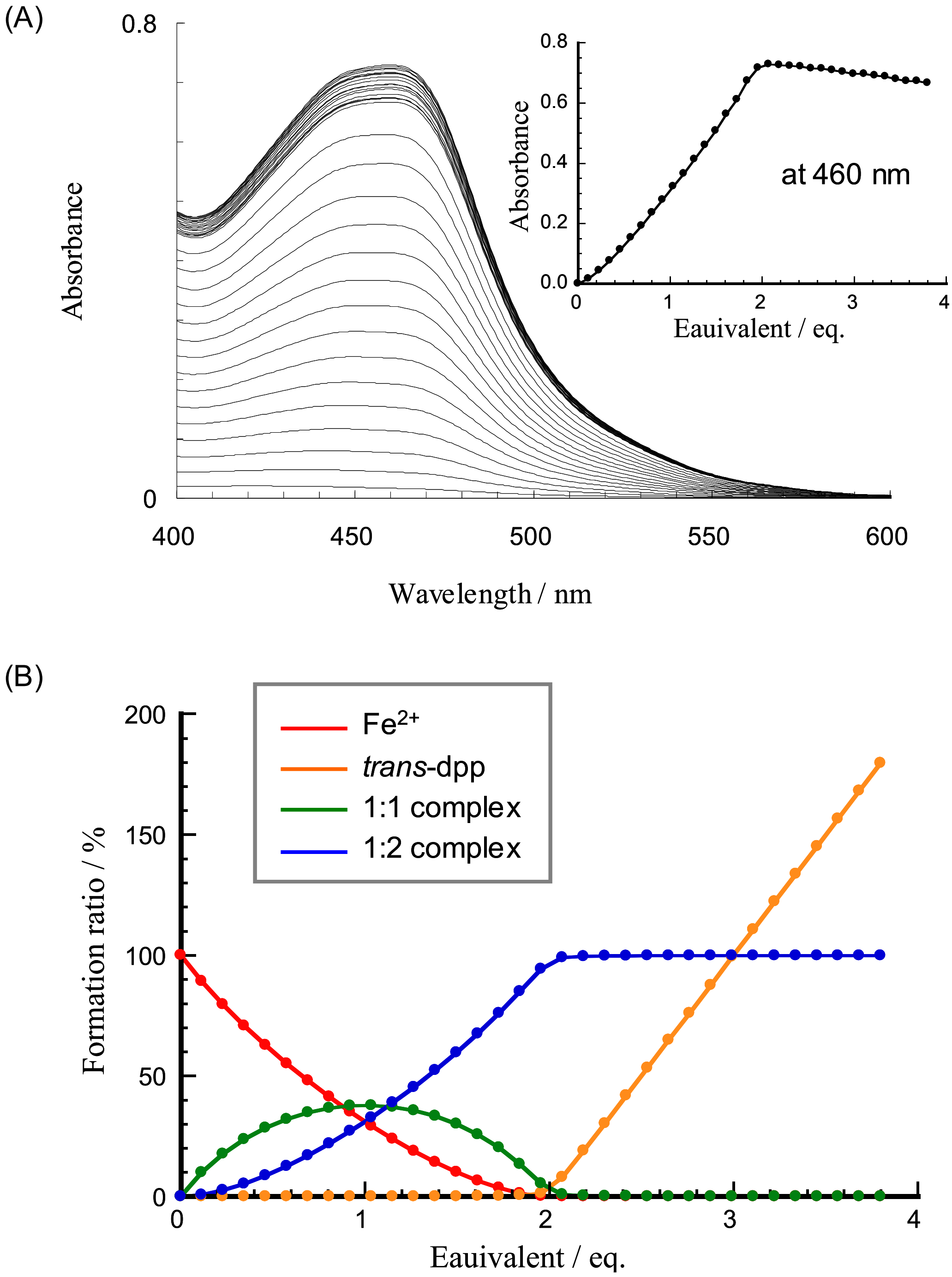

Figure S–3–2. (A) Spectrophotometric titration of $Fe(BF_4)_2 \cdot 6H_2O$ with *E*-**1** in acetone. The concentration of $Fe(BF_4)_2 \cdot 6H_2O$ is 1.34×10^{-4} M and of *E*-**1** is 1.85×10^{-3} M. Inset: absorbance at 500 nm as a function of added equivalent of the ligand. (B) Corresponding distributions of Fe^{2+} (red), *E*-**1** (orange), 1:1 complex (green), 1:2 complex (blue) as a function of added equivalents of the ligand.

S–4 Photoisomerization behaviors in solution

Photoisomerization behaviors of *E*-2 in acetone upon irradiation with 436 nm light

As in the case of *Z*-**2**, 1.0 equivalent of excess free ligand, *E*-**1**, was coexisted in an acetone solution of *E*-**2** to avoid the formation of dissociated complexes. UV–vis spectra of *E*-**2** before and after irradiation are shown in ***Figure S–4–1***. The initial absorption band in the visible region, which is attributed to an MLCT band, did not show any spectral change upon irradiation, revealing that the absence of any photoreaction. The maximum change in absorbance after irradiation for longer than 4 h was within 1%.

Dependence of Wavelengths on Photoisomerization of Ligands and Their Iron(II) and Zinc(II) Complexes

Photoisomerization behaviors of *E*- and *Z*-**1**, and their iron(II) and zinc(II) complexes in acetonitrile were also investigated by the use of UV–vis spectroscopy. In these measurements, excess free ligands were not added to the solution of complexes. Spectra in their photostationary state (PSS) obtained by irradiation with various wavelengths light were well matched to weighed averages of spectra for their *E*- and *Z*-isomers. Consequently, the *E*-isomer ratio in each PSS was determined by their spectral fitting analyses based on least squares methods. Their *E*-isomer ratios in PSS are listed in ***Table S–4–1***.

Figure S–4–2 shows photoisomerization behavior of *Z*-**1**. Irradiation with 313 nm light, which corresponds to the exicitation of almost degenerate π–π^* and n–π^* transitions,[12] led to a *Z*-rich state within a few minutes. A *E*-isomer ratio in this state, 0.30, is almost the same as the ratio of molar extinction coefficients at this wavelength between *Z*- and *E*-**1**, 0.28, indicating that quantum yields for *Z*-to-*E* and *E*-to-*Z* photoisomerization are similar.[13] A spectrum obtained by further irradiation with 313 nm light showed further spectral changes, indicating that some side-reactions other than photoisomerization, like cyclization reactions, commonly observed in stilbene derivatives to form their 4*a*,4*b*-dihydrophenanthrene (DHP) derivatives,[14] would occur.

Photoisomerization behavior for $[\mathrm{Zn}(Z\text{-}\mathbf{1})_2](\mathrm{BF}_4)_2$ was found to be similar to that of *Z*-**1** as shown in ***Figure S–4–3***. As in the case of *Z*-**1**, irradiation with 313 nm light led to a PSS rich in *cis*-isomer within a few minutes. A *E*-isomer ratio in its PSS, 0.33, is almost the same as the ratio of molar extinction coefficients at this wavelength between *Z*- and *E*-isomers, 0.32. Irradiation with 365 nm light led to its PSS somewhat richer in its *Z*-isomer, due to large differences in molar extinction coefficients at this wavelength.

Figure S–4–4 shows photoisomerization behavior of *Z*-**2**. While the peak position and the molar extinction coefficient in its degenerate π–π^* and n–π^* band are similar to those of $[\mathrm{Zn}(Z\text{-}\mathbf{1})_2](\mathrm{BF}_4)_2$, irradiation with 313 nm light led to a *E*-rich state. A *E*-isomer ratio in its PSS, 0.58, is higher than the ratio of molar extinction coefficients at this wavelength between *Z*- and *E*-isomers, 0.32. This result implies a contribution of an internal conversion from its π–π^* (or n–π^*) excited state to its MLCT excited state, making a quantum yield for *Z*-to-*E* photoisomerization higher than that for *E*-to-*Z* photoisomerization. As the irradiation wavelengths get longer, *E*-isomer ratios in their PSS become larger, to reach 0.98 upon irradiation with 436 nm light. This result indicates that *E*-isomer also dominantly forms in acetonitrile as is observed in acetone, while the value is slightly less than unity. Solvent effects and/or the effect of ligand dissociation would have caused this small difference.

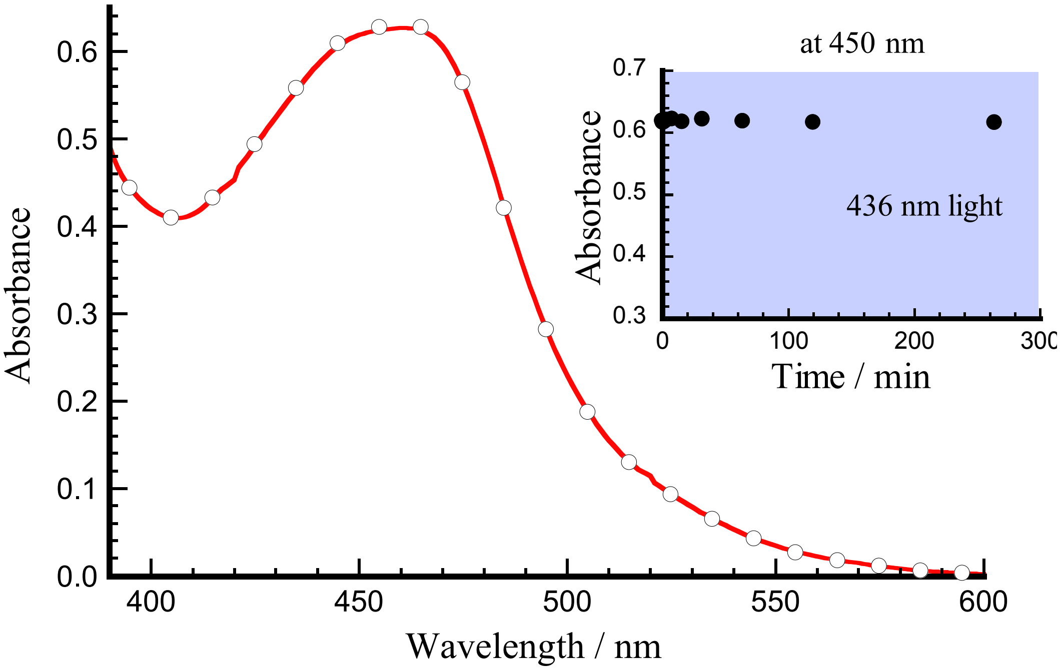

Figure S–4–1. A UV–vis spectrum of *E*-**2** in acetone (a red line, 1.06×10^{-4} M), containing 1.0 equivalent of *E*-**1**, and a spectrum in its PSS upon irradiation with 436 nm light (black circles) at 295 K. Inset: time-course changes in absorbance at 450 nm.

Table S–4–1. Relationship between Irradiation Wavelengths and *E*-isomer Ratios of Ligands and Complexes in Acetonitrile at 295 K

Wavelength/nm	*E*-isomer ratio in PSS[a]		
	E-**1** and *Z*-**1**	$[Zn(E\text{-}\mathbf{1})_2](BF_4)_2$ and $[Zn(Z\text{-}\mathbf{1})_2](BF_4)_2$	*E*-**2** and *Z*-**2**
313	0.30[b]	0.33	0.58
365	0.21	0.12	0.84
436	–	–	0.98

[a] Determined by their spectral fitting analyses based on least-squares methods. [b] Some side-reactions were spectroscopically detected by continuous irradiation for a long period.

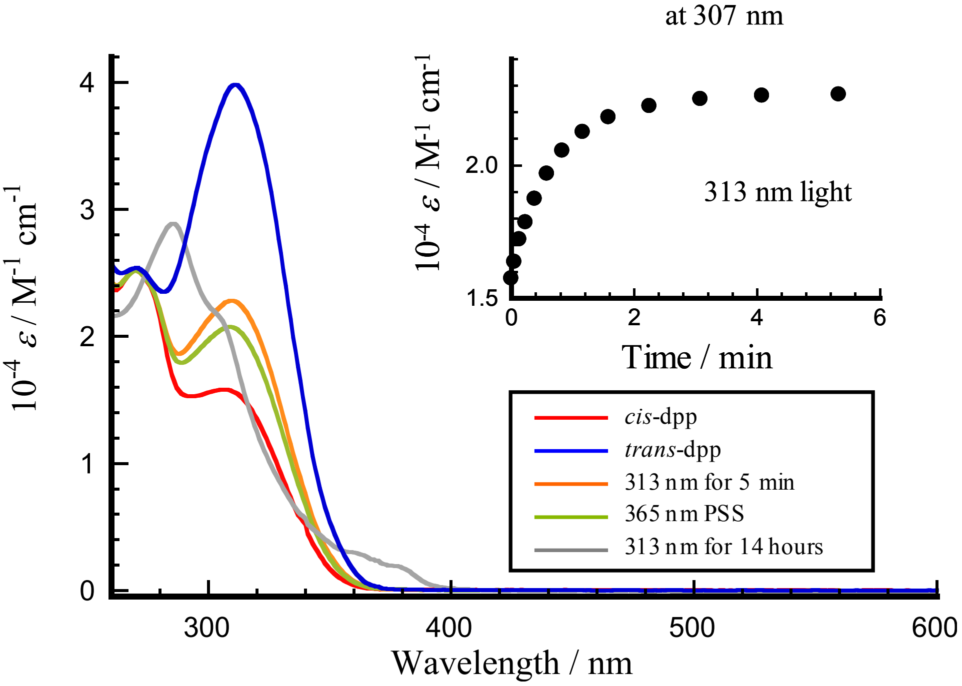

Figure S–4–2. UV–vis spectra of *Z*-**1** (a red line, 1.91×10^{-5} M) and *E*-**1** (a blue line, 2.08×10^{-5} M) in acetonitrile, and a spectrum in its PSS upon irradiation with 365 nm light (a yellow–green line) to the following solution of *Z*-**1** at 295 K. Spectra upon irradiation with 313 nm for 5 min (an orange line) and 14 h (a gray line) to the following solution of *Z*-**1** are also shown. Inset: time-course changes in a molar extinction coefficient at 307 nm upon irradiation with 313 nm light.

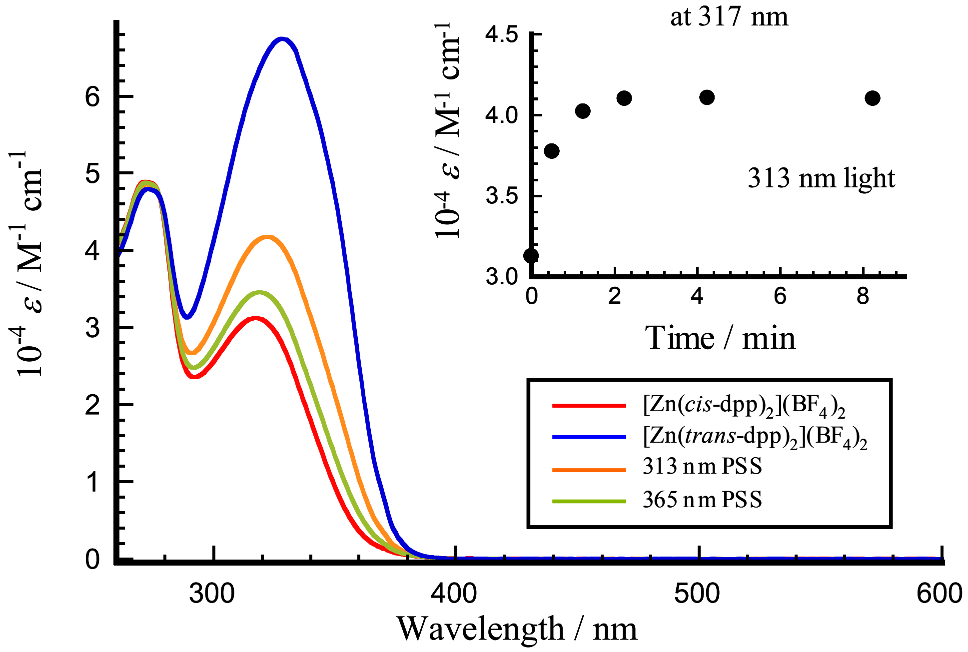

Figure S–4–3. UV–vis spectra of [Zn(*Z*-**1**)$_2$](BF$_4$)$_2$ (a red line, 1.96 × 10^{-5} M) and [Zn(*E*-**1**)$_2$](BF$_4$)$_2$ (a blue line, 2.00 × 10^{-5} M) in acetonitrile, and spectra in their PSS upon irradiation with 313 (an orange line) and 365 nm light (a yellow–green line) to the following solution of [Zn(*Z*-**1**)$_2$](BF$_4$)$_2$ at 295 K. Inset: time-course changes in a molar extinction coefficient at 317 nm upon irradiation with 313 nm light.

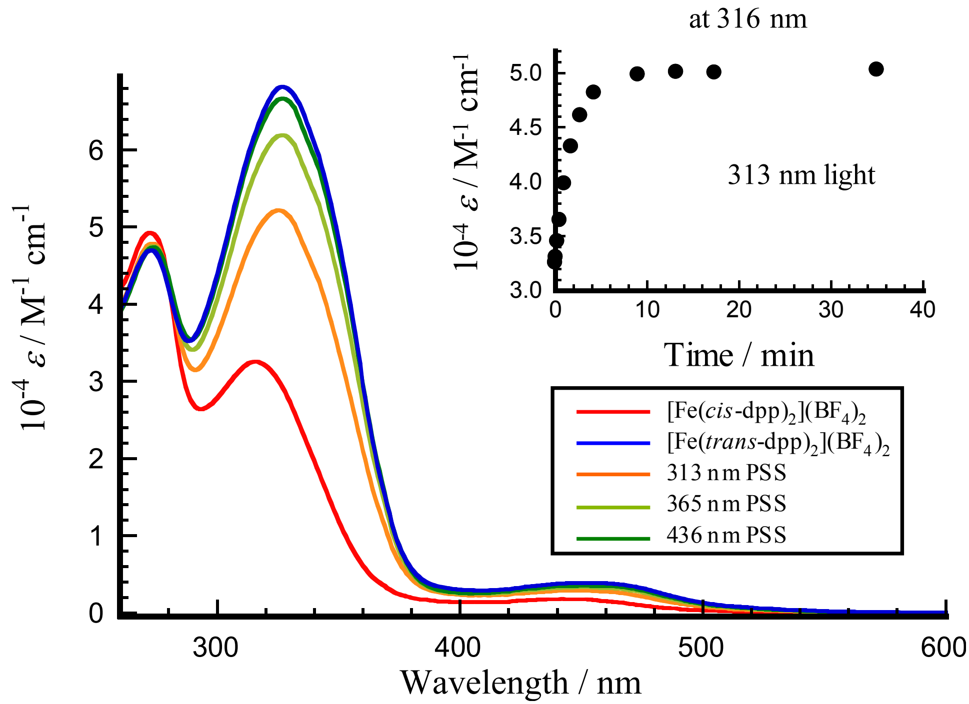

Figure S–4–4. UV–vis spectra of *Z*-**2** (a red line, 1.98 × 10^{-5} M) and *E*-**2** (a blue line, 1.75 × 10^{-5} M) in acetonitrile, and spectra in their PSS upon irradiation with 313 nm (an orange line), 365 nm (a yellow–green line), and 436 nm light (a green line) to the following solution of *Z*-**2** at 295 K. Inset: time-course changes in a molar extinction coefficient at 316 nm upon irradiation with 313 nm light.

S–5 Comparison of IR and UV-vis spectra before and after irradiation

In the crystal lattice of compounds the molecules have only a very small freedom of movement, because they are as closely packed as possible. In solids, *Z–E* photoisomerizations [15] are estimated to occur by a volume-conserving *Z–E* isomerization mechanism (Hula-Twist mechanism).[16] In this model, only one C–H unit undergoes out-of-plane translocation, while remaining portions of the molecule slide along in the general direction of the molecule.

IR spectra before and after irradiation in a pelletized sample

As shown in ***Figure S–5–1***, the IR spectrum of *Z*-**2** after irradiation for 300 minutes excellently matches that of *E*-**2** in just propotion, and shows no characteristic peak of *Z*-**2**. The result suggests that one-way *Z*-to-*E* photoisomerization by irradiation with visible light is also active even in solid.

Determination of a ratio of formed *E*-isomer in the irradiated microcrystals of *Z*-2

The color of *Z*-**2** gradually changed from yellow to red upon irradiation, and the color change was completed after irradiation for 70 h. Further irradiation did not influence the appearance. The sample irradiated for 115 h was palletized with KBr, whose IR spectrum was almost identical to *E*-**2** (***Figure S–5–2***). The ESI-TOF mass of the irradiated sample did not show any peak other than those for $[\mathrm{Fe}(X\text{-}\mathbf{1})_2]^{2+}$ ($X = Z$, E),[17] revealing the absence of any side-reaction such as a dimerization reaction of the ethylenyl moiety.

The irradiated *Z*-**2** was dissolved in acetonitrile and a UV-vis spectrum of the solution was measured.

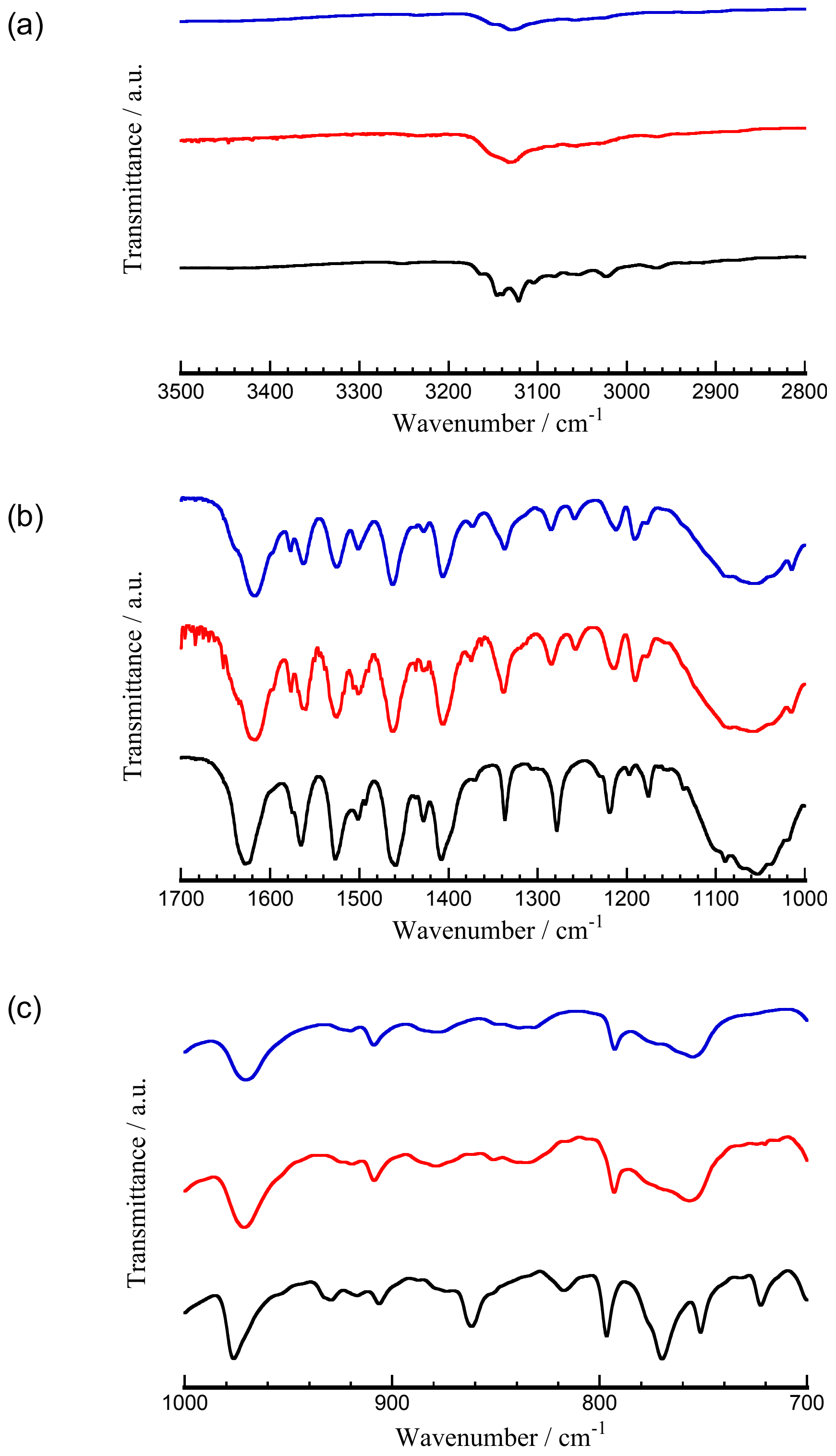

Figure S–5–1. IR spectra of *Z*-**2** before irradiation (black lines), after irradiation with 436 nm light for 300 min in the KBr pelletized state (red lines), and *E*-**2** (blue lines) in the 3500–2800 cm^{-1} (a), 1700–1000 cm^{-1}, and 1000–700 cm^{-1} regions (c).

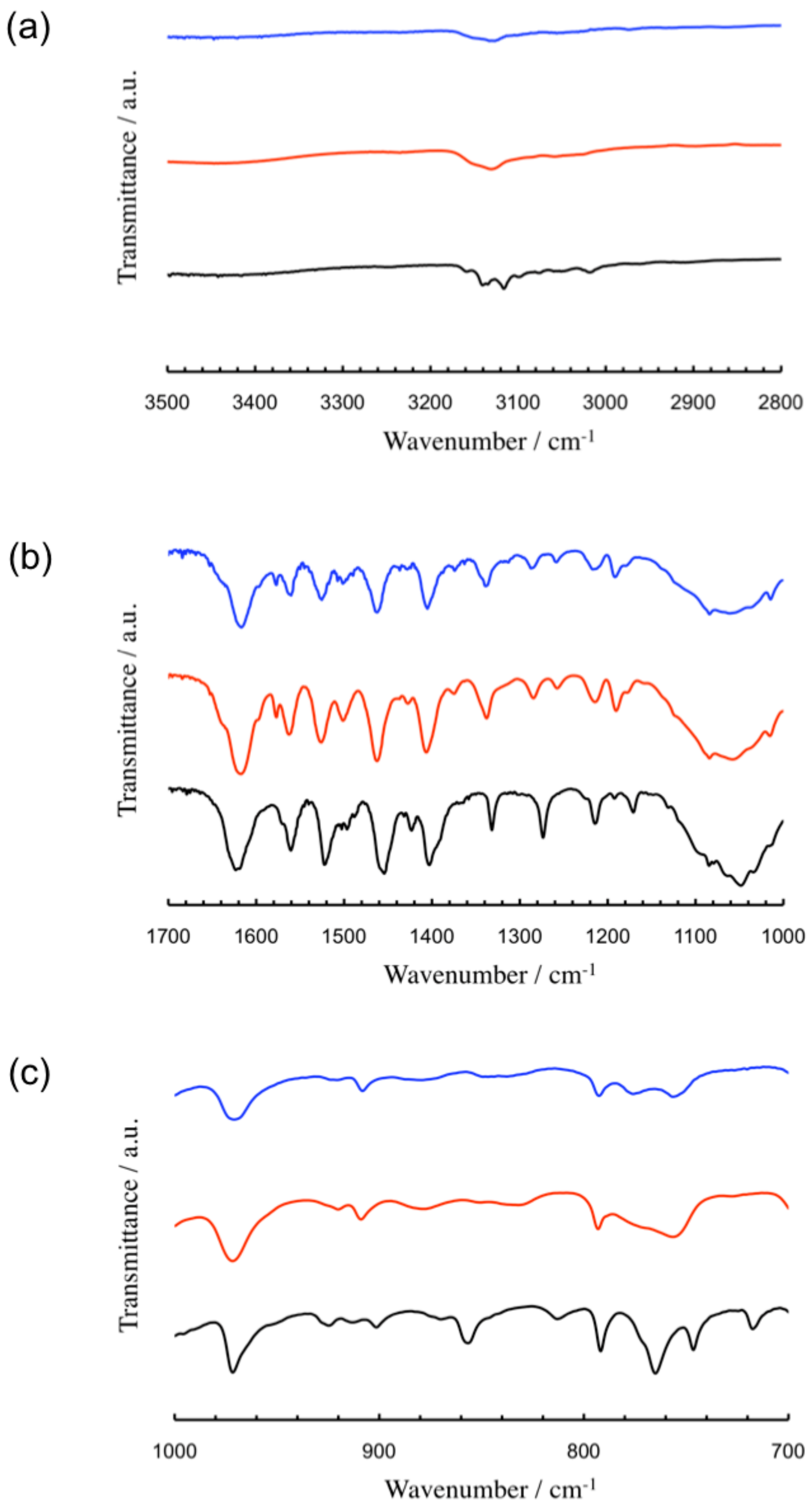

Figure S–5–2. IR spectra of *Z*-**2** before irradiation (black lines), after irradiation with visible light (> 420 nm) for 115 h in the microcrystalline solid state (red lines), and *E*-**2** (blue lines) in the 3500–2800 cm^{-1} (a), 1700–1000 cm^{-1}, and 1000–700 cm^{-1} regions (c).

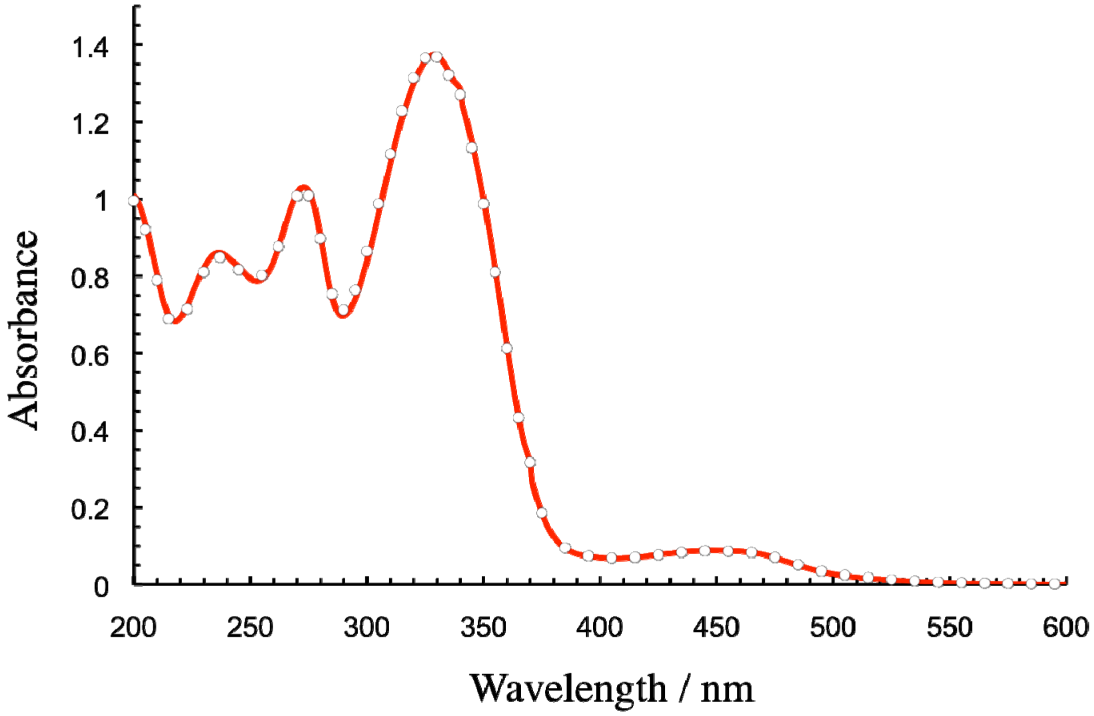

Figure S–5–3. A UV-vis spectrum of *Z*-**2** in acetonitrile (red line, 2.00 × 10^{-5} M) after irradiation with visible light (> 420 nm) for 115 h in the microcrystalline solid state. The simulated spectrum given in circles were for a mixture of *Z*-2 and *E*-2 in the ratio of 12 : 88.

S–6 References

[1] J. Elhaïk, C. M. Pask, C. A. Kilner, M. A. Halcrow, *Tetrahedron* **2007**, *63*, 291–298.

[2] S. Gronowitz, K. Stenhammer, L. Svensson, *Heterocycles* **1981**, *15*, 947–959.

[3] a) M. Tsukamoto, M. Schlosser, *Synlett* **1990**, 605–608; b) S. Jaganathan, M. Tsukamoto, M. Schlosser, *Synthesis* **1990**, 109–111.

[4] Higashi (1999). Programs for Absorption Correction. Rigaku Corporation, Tokyo, Japan.

[5] A. Altomare, M. C. Burla, M. Camalli, G. L. Cascarano, C. Giacovazzo, A. Guagliardi, A. G. G. Moliterni, G. Polidori, R. Spagna, *J. Appl. Cryst.* **1999**, *32*, 115–119.

[6] M. C. Burla, R. Caliandro, M. Camalli, B. Carrozzini, G. L. Cascarano, L. De Caro, C. Giacovazzo, G. Polidori, R. Spagna, *J. Appl. Cryst.* **2005**, *38*, 381–388.

[7] G. M. Sheldrick, *SHELX-97. A Program for Crystal Structure Analysis*, release 97-2, WinGX Version; University of Göttingen, Germany, **1997**.

[8] L. J. Farrugia, WinGX suit for small-molecular single-crystal crystallography. *J. Appl. Cryst.* **1999**, *32*, 837–838.

[9] a) R. A. Binstead, B. Jung, A. D. Zuberbühler, SPECFIT/32 for Windows, Spectrum Software Associates, Marlbrough, MA; b) H. Gampp, M. Maeder, C. J. Meyer, A. D. Zuberbühler, *Talanta* **1985**, *32*, 95-101.

[10] M. Nihei, L. Han, H. Oshio, *J. Am. Chem. Soc.* **2007**, *129*, 5312–5313.

[11] B. Straub, W. Linert, V. Gutmann, R. F. Jameson, *Monat. Chem.* **1992**, *123*, 537–546.

[12] G. Marconi, G. Bartocci, U. Mazzucato, A. Spalletti, F. Abbate, L. Angeloni, E. Castellucci, *Chem. Phys.* **1995**, *196*, 383–393.

[13] D. G. Whitten, M. T. McCall, *J. Am. Chem. Soc.* **1969**, *91*, 5097–5103.

[14] D. H. Waldeck, *Chem. Rev.* **1991**, *91*, 415–436.

[15] a) M. D. Cohen, M. J. Schmidt, F. I. Sonntag, *J. Chem. Soc.* **1964**, 2000–2041; b) Kaupp, *Comprehensive Supramolecular Chemistry*, *Vol.* 8 (Eds: Davies, J. E. D.; Ripmeester, J. A.), Elsevier, Oxford, **1995**, pp 382–411; c) G. Kaupp, M. Haak, *Angew. Chem. Int. Ed.* **1996**, *35*, 2774–2777.

[16] a) R. S. H. Liu, G. S. Hammond, *Chem. Eur. J.* **2001**, *7*, 4536–4544; b) K. Tanaka, T. Hiratsuka, S. Ohba, M. R. Naimi-Jimal, G. Kaupp, *J. Phys. Org. Chem.* **2003**, *16*, 905–912.

[17] ESI-TOF mass (positive, acetonitrile): *m*/*z* = 341.05 $[M]^{2+}$, calcd for $C_{38}H_{30}FeN_{10}$, 341.10.